BIOCHEMISTRY
including biophysical chemistry & molecular biology

Article

pubs.acs.org/biochemistry

Extracellular Juxtamembrane Segment of ADAM17 Interacts with Membranes and Is Essential for Its Shedding Activity

Stefan Düsterhöft,[†,#] Matthias Michalek,[‡,#] Felix Kordowski,[§,#] Mirja Oldefest,[†] Anselm Sommer,[§] Jona Röseler,[†] Karina Reiss,[§] Joachim Grötzinger,[*,†] and Inken Lorenzen[†]

[†]Institute of Biochemistry and [‡]Zoological Institute, Comparative Immunobiology, Christian-Albrechts-University Kiel, Olshausenstrasse 40, 24098 Kiel, Germany

[§]Department of Dermatology and Allergology, University Hospital Schleswig-Holstein, Campus Kiel, Schittenhelmstrasse 7, 24105 Kiel, Germany

ABSTRACT: A wide variety of biological processes including differentiation, regeneration, and cancer progression are regulated by shedding of membrane-anchored proteins. One of the major sheddases is A Disintegrin And Metalloprotease-17 (ADAM17) whose extracellular region consists of a pro-, a catalytic, a disintegrin-, and a membrane-proximal domain (MPD) as well as a short juxtamembrane segment of 17 amino acid residues that has been named "Conserved ADAM-seventeeN Dynamic Interaction Sequence" (CANDIS). This segment is involved in substrate recognition. Key mediators of inflammation including interleukin-6 receptor (IL-6R) and tumor necrosis factor (TNF-α) are substrates of ADAM17. The shedding activity of ADAM17 is regulated by the conformation of the membrane-proximal domain preceding the CANDIS segment. Here, we show that CANDIS, besides being involved in substrate recognition, is able to interact with lipid bilayers in vitro and that this property could be involved in regulating ADAM17 shedding activity.

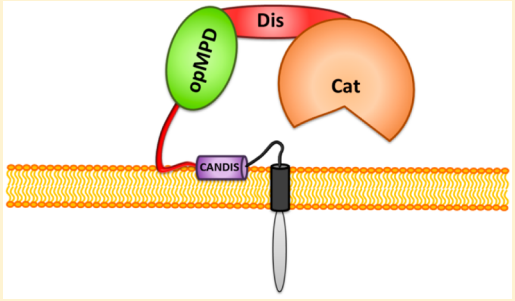

Many biological processes are regulated by irreversible proteolytic steps. One of these processes is the extracellular proteolytic cleavage of membrane-bound proteins resulting in the release of soluble agonists or antagonists. Members of the so-called A Disintegrin And Metalloproteases (ADAMs) family are the major proteases responsible for these ectodomain shedding. The vitally important ADAM17 is a type-I transmembrane protein that is involved in developmental, regenerative, and immunological responses, but is also associated with uncontrolled inflammation and cancer progression.[1−5] More than 75 substrates have been identified to be shed by this enzyme,[6] including proforms of growth factors, such as transforming growth factor TGF-α,[1] pro-inflammatory cytokines such as tumor necrosis factor-α (TNF-α),[4,7] as well as the cytokine receptors TNF-α receptor I (TNFRI),[8] the interleukin-1 receptor II (IL-1RII),[8] and the interleukin-6 receptor (IL-6R).[9] Shedding of these molecules not only provides the possibility for down-regulation, but also for initiating or inhibiting autocrine or paracrine signaling via soluble proteins. Shedding of proTNF-α results in the generation of the pro-inflammatory soluble cytokine. Cleavage of TNFRI desensitizes TNFRI expressing cells for TNF-α.[10,11] In addition, the soluble TNFRI ectodomain acts as an antagonist of TNF-α signaling mediated by its membrane-bound form. Both processes result in immunosuppressive and anti-apoptotic consequences of TNFRI shedding.[11] In contrast, release of the IL-6R generates an agonist of IL-6 signaling, the soluble IL-6R (sIL-6R). Whereas membrane-bound IL-6R is associated with regenerative processes, the sIL-6R initiates pro-inflammatory responses by a process called trans-signaling.[12−14] ADAM17 and its closest relative ADAM10 are atypical members of the ADAM family as they do not possess the classical EGF-like and cysteine-rich domain of other ADAM family members in their ectodomain. Instead, the disintegrin domain is followed by a membrane-proximal domain (MPD) and a small stalk region. The highly conserved ADAM17 stalk region has been named CANDIS (Conserved ADAM seventeeN Dynamic Interaction Sequence).[15] ADAM17 mediated shedding is negatively regulated by extracellular protein disulfide isomerases (PDI).[16,17] Furthermore, it has been shown that the CXXC-motif of MPD is crucial for the enzyme activity and represents a target for redox modifications.[18,19]

Interestingly, the isolated MPD of ADAM17 has been shown to exist in two conformations (a closed and an open conformation) dependent on their disulfide pattern.[20] The conformations of the MPD seem to be directly connected to shedding activity. It might be assumed that these changes in conformation might also occur in vivo and might explain the PDI-dependent decrease in ADAM17 activity. This regulatory switch is in vitro mediated by protein disulfide isomerase.[20] The ability of CANDIS to specifically bind ADAM17 substrates is in

Received: May 12, 2015
Revised: September 7, 2015
Published: September 8, 2015

DOI: 10.1021/acs.biochem.5b00497
Biochemistry 2015, 54, 5791−5801

turn regulated by the conformation of the preceding MPD in vitro.[15] CANDIS is able to interact with substrates, when the MPD is in the open form, but substrate binding does not occur with the closed form suggesting that the binding site in CANDIS is possibly concealed when the MPD is in the inactive state.[21] It has been shown that proteolytic cleavage of some ADAM17 substrates, for instance, TNF-α and IL-6R, is sequestered by cholesterol-rich lipid rafts, whereas the processing of others, such as jagged1, is not.[22−24] Interestingly, cholesterol depletion of cells leads to an activation of ADAM17.[25] These data point to a regulatory role of the membrane composition on the ADAM17 activity.[26] Here, we show that CANDIS can bind to membranes and that this property depends on lipid composition. Interestingly, mutations in the hydrophobic side of CANDIS within the full-length molecule lead to a decreased shedding activity suggesting that membrane binding might be an important step in the activation mechanism of ADAM17.

MATERIALS AND METHODS

Peptides. The following peptides were used: CANDIS = RVQDVIERFWDFIDQLS_GSGSGK, pA10 = VDADGPLARLKKAIFSP_GSGSGK, control peptide (cp) = DQWRVVQIEFDIDLFRS_GSGSGK. All peptides were purchased from Biosyntan GmbH (Berlin, Germany) or peptides&elephants GmbH (Potsdam, Germany). Lipids were purchased from Avanti Polar Lipids (Alabaster, AL, USA).

Vesicle Preparation. For vesicle preparation lipid mixtures composing POPC/POPS (75/25% molar ratio), POPC (100%), POPC/POPS/cholesterol (52.5/17.5/30% molar ratio), and POPC/cholesterol (70/30% molar ratio) were dissolved in chloroform and subsequently evaporated under a nitrogen stream to obtain a thin lipid film. Residual solvent was removed by lyophilization, followed by 2 h shaking in 20 mM Tris/HCl, pH 7.4 for rehydration. The suspension was subjected to three cycles of freezing in liquid nitrogen and thawing in a water bath of 37 °C. Finally, small unilamellar vesicles (SUV) were produced by extrusion 21 times through 50 nm polycarbonate membranes (Avestin, Mannheim, Germany).

CD Spectroscopy. Circular dichroism spectroscopy was performed on a Jasco J-720 CD spectrometer (Jasco, Tokyo, Japan) with a bandwidth of 1 nm and a cuvette of 1 mm path length. The spectropolarimeter was calibrated according to Chen and Yang.[27] The peptide concentrations were 20 μM in 20 mM Tris/HCl, pH 7.4, and SUVs were added to P/L ratios as indicated. Four scans with a scan speed of 20 nm/min were averaged, and the CD signal of the buffer and lipids was subtracted subsequently. The dilution factor was recalculated after each experiment. Analysis of spectra was performed using Origin 6.0, and helical contents were calculated using the CONTIN/LL algorithm.[28] Upon lipid vesicle titration the CD chromatograms were used to analyze the membrane dissociation constant as described previously.[29] For this, the fraction of membrane-associated peptide was calculated from conformational changes exemplified by

$$\text{Bound peptide}\ (\%) = ([\Theta] - [\Theta]_0)/([\Theta]_{max} - [\Theta]_0)$$

where $[\Theta]$ is the measured ellipticity at 222 nm of the sample, $[\Theta]_0$ is the baseline of the buffer with and without lipids of each titration step, and $[\Theta]_{max}$ is the maximal ellipticity at 222 nm upon peptide-lipid saturation. The spectral data were fitted by equations for low and high affinity, showing consistent K_d values for the CANDIS−membrane interaction.

Fluorescence Spectroscopy. Tryptophan-emission fluorescence measurements were performed on a Hitachi F-2500 fluorescence spectrometer (Tokyo, Japan) with an excitation wavelength of 290 nm at 20 °C. SUV lipid mixtures were added from stock solutions of 10 mM to a solution of CANDIS peptides (1 μM final concentration) in 20 mM Tris/HCl, pH 7.4 into quartz cuvettes of 1 cm path length (Hellma Analytics, Müllheim, Germany). Emission and excitation bandwidth were set to 2.5 and 5 nm, respectively, with the photomultiplier tube voltage of 700 V. Emission spectra were recorded after short incubation from 300 to 400 nm with a scanning speed of 60 nm/min and averaging three scans. Spectra were corrected for baseline and dilution after adding lipid vesicles for each titration step. Fluorescence intensities were calculated from the area under the emission curve of peptide (I_0) and peptide−lipid mixtures (I). The binding of CANDIS peptides to SUVs of various lipid compositions was analyzed by successive lipid vesicle addition and was described by the dissociation constants (K_d), derived from previous observations.[29] For fitting the spectral data, equations for low or high affinity were applied. For low affinity binding the following equation was used:

$$I = (I_0 + I_{max}K_a[L_{tot}])/(1 + K_a[L_{tot}])$$

where I_{max} is the fluorescence intensity after binding saturation, $[L_{tot}]$ is the total lipid concentration and $[K_a]$ the association constant, which gives K_d $(1/K_a)$. For high affinity, the quadratic equation was applied:

$$I = I_0 + [P_L](I_{max} - I_0)/[P_{tot}]$$

$$[P_L] = \{(K_d + [P_{tot}] + [L_{tot}]) - \{(K_d + [P_{tot}] + [L_{tot}])^2 - 4[P_{tot}][L_{tot}]\}^{1/2}\}/2$$

where $[P_L]$ is the concentration of the peptide−lipid complex, $[P_{tot}]$ is the total peptide concentration, and K_d is the dissociation constant. The determined K_d values were consistent for both equations applied. The data of the tryptophan emission were fitted using Origin 6.0.

Antibodies. Rabbit anti-HA was from Sigma-Aldrich, Germany or Cell Signaling, USA, rabbit anti-ADAM17 used for Western blotting was from Millipore, Germany, rabbit K133 anti-ADAM17 was from the Department of Immunology, Group Koch-Nolte, UKE, Hamburg, Germany, rabbit IgG1 was from Southern Biotechnology, USA and antirabbit Alexa Fluor 488 detection antibody was from Life Technologies, Germany, and murine anti-β-actin C4 was from Santa Cruz Biotechnologies, USA.

Expression Vectors. The expression vectors for ADAM17 wild-type and the expression constructs for alkaline phosphatase (AP)-tagged TGFα (TGFα-AP) were from C. Blobel (Hospital for Special Surgery, New York, USA). The AP-proTNFα expression plasmid was provided by Athena Chalaris (Institute of Biochemistry, Christian-Albrechts-University Kiel, Germany).

Generation of the Mutated ADAM17 Plasmids. The mutated ADAM17 plasmids ADAM17EE (F652E F655E substitutions) and ADAM173Q (D647Q E650Q D654Q substitutions) were generated by site-directed mutagenesis with the Quikchange II site-directed mutagenesis kit following the manufacturer's instruction (Agilent technologies, USA) using the ADAM17 wild-type (A17WT) plasmid as template

DOI: 10.1021/acs.biochem.5b00497
Biochemistry 2015, 54, 5791−5801

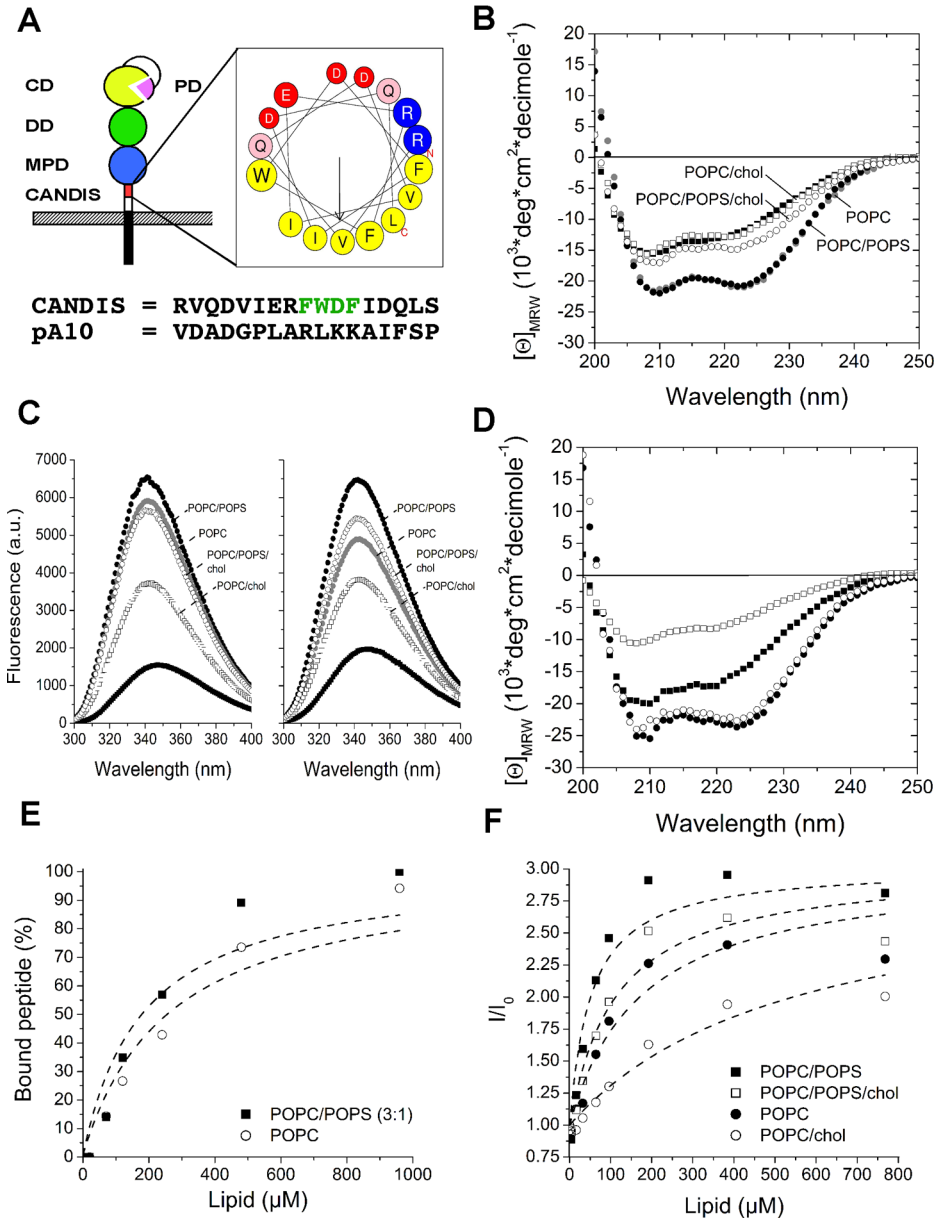

Figure 1. (A) Schematic representation of ADAM17. PD: pro-domain; CD: catalytic domain; DD: disintegrin domain; MPD: membrane-proximal domain; CANDIS: A Conserved ADAM seventeeN Dynamic Interaction Sequence. The helical wheel of CANDIS is presented where yellow colored circles represent hydrophobic, red and blue are charged and pink are hydrophilic amino acids. Amino acid sequences of CANDIS and the corresponding region of ADAM10. The FDWF motive is highlighted in green. (B) CD spectra of the CANDIS peptide in the absence (filled squares) and the presence of SUVs composed of various lipid compositions in 48 fold higher concentrations compared with the peptide (P/L ratio of 1:48). C (left) Tryptophan emission spectra of CANDIS (1 μM) in the absence and presence of SUVs (300 μM) composed of different lipid compositions. (right) The same experiments were also performed in the presence of 150 mM NaCl. (D) CD spectra of the CANDIS peptide without salt (filled squares) and with 150 mM NaCl (empty square) in the absence of SUVs. In the presence of POPC/POPS (75:25 molar ratio) containing SUV vesicles, CD spectra of CANDIS were collected without salt (empty circle) and with 150 mM NaCl (filled circle). (E) The determination of dissociation constants were derived from the increase of ellipticities at 222 nm of the CD signal upon stepwise addition of SUVs composed of POPC or POPC/POPS (75/25% molar ratio). (F) The binding isotherms of CANDIS upon stepwise addition of SUVs composed of POPC, POPC/chol (70/30% molar ratio), POPC/POPS (75/25% molar ratio), or POPC/POPS/chol (52.5/17.5/30% molar ratio) were followed by the fluorescence intensity increase of tryptophan emission fluorescence spectroscopy. Binding curves were fitted as described in the Materials and Methods.

and primers ordered from Sigma, Germany. Successful mutation was verified by sequencing (Seqlab, Germany). ADAM17 CANDIS chimera (ADAM17p10) was created by overlapping PCR whereby CANDIS (K643-Q658) was replaced by L648-I662 of murine ADAM10.

Cell Culture, Transfection, and Alkaline Phosphatase Ectodomain Shedding Assay. ADAM10/17-deficient mouse embryonic fibroblasts (MEFs) were described previously[30] and were transfected using the Turbofect Transfection Reagent (Thermoscientific, Germany) with plasmids containing ADAM17 wild-type, ADAM17EE mutant, or ADAM173Q mutant and plasmids containing alkaline phosphatase coupled to TGF-α. The control condition was MEFs transfected with TGF-α-AP plasmid alone. For Western blotting, cells were

DOI: 10.1021/acs.biochem.5b00497
Biochemistry 2015, 54, 5791−5801

lysed after 24 h. For shedding assays 24 h after transfection, MEFs were washed with DMEM, which was renewed after 1 h and treated or not treated with phorbol 12-myristate 13-acetate (PMA, 200 ng/mL, Sigma-Aldrich, Germany) for 2 h or ionomycin (Iono, 1 μM, Calbiochem, Germany) for 30 min. Afterward, supernatants and cell lysates were collected and measured for alkaline phosphatase activity by absorption at 405 nm after incubation with the alkaline phosphatase substrate 4-nitrophenyl phosphate (Sigma-Aldrich, Germany). The values were baseline-corrected with the AP-activity of the controls. The relative-AP activity in the supernatant is shown in comparison with the total AP activity of supernatant including cell lysates, normalized to the stimulated wild-type ADAM17 cells. For shedding assays, the cells were lysed in buffer containing 2.5% Triton-X, 10 mM 1,10-phenanthroline, and 1 mM EDTA in water. In the case of TNF-α and TGF-α shedding by ADAM17 variants or by ADAM17 CANDIS chimera experiments was performed as described previously[17] with the following exceptions: the metalloprotease inhibitor marimastat (10 μM) was added to the culture medium of TNF-α transfected ADAM10/17-deficient MEFs 2 h post transfection and 15 min before stimulation of TGF-α transfected cells. Briefly, cells were cotransfected with AP-tagged substrates and either empty vector, wild-type ADAM17, or different ADAM17 variants or chimera in duplicates. Twenty-four hours later, cells were washed three times with warm PBS, and ADAM17 was stimulated by the addition of 100 nM PMA or was stimulated by 100 nM PMA in the presence of 10 μM marimastat. Two hours later, supernatant and cell lysates were harvested and AP activities were measured. The ratios of supernatant against lysate were normalized against the sample treated with the metalloprotease inhibitor marimastat. These ratios were normalized by setting the activity of PMA stimulated cells transfected with wild-type ADAM17 to 100% of shedding activity. Expression levels of ADAM17 variants were analyzed from the cell lysates treated with PMA and marimastat by usage of the C-terminal HA-tag.

Western Blot Analysis. Cells were lysed on ice in lysis buffer (5 mM Tris, 1 mM EGTA, 250 mM saccharose, Triton-X100 (1%), 1,10-phenanthroline (10 mM), and protease inhibitors (Roche, Germany)). Comparable amounts of protein were separated on 7.5% sodium dodecyl sulfate polyacrylamide gels, and transferred onto polyvinylidene difluoride (PVDF) membranes (PEQLAB Biotechnologie, Germany). These were treated with 5% skim milk in TBS with 0.1% Tween, subsequently incubated with primary antibodies and washed in 0.1% Tween-TBS. Bound primary antibodies were detected with peroxidase-conjugated goat antimouse or goat antirabbit antibodies (Dianova, Germany) using the ECL detection system (GE Healthcare, Germany) and a Fusion FX7 imaging system (PEQLAB Biotechnologie, Germany).

Flow Cytometry Analysis. For analyzing the surface expression of the ADAM17 proteins, ADAM10/17-deficient mouse embryonic fibroblasts were transfected with the respective plasmid and 24 h later harvested with Accutase (Innovative Cell Technologies, CA, USA). Cells were blocked with 3% BSA in PBS and afterward incubated with 1 μg/1 $\times$ 10^6 cells Fc-Block in buffer (purified rat anti-mouse CD16/CD32 from BD, Germany). Thereafter cells were either not stained or stained with K133 (10 μg/mL) anti-ADAM17 antibody or rabbit IgG1 (10 μg/mL) antibodies as isotype control for 1 h at 4 °C. Afterward the cells were washed and incubated for 1 h with 6.6 μg/mL antirabbit Alexa Fluor 488 detection antibody (Life Technologies, Germany), washed again, and analyzed by flow cytometry with Fortessa flow cytometer (BD, Germany). The flow cytometry data were analyzed by using the software FlowJo 8.7.3. FACS buffer contained 2 mM EDTA, 1% BSA in PBS.

Coupling of Peptides with Fluorophore. 0.5 mM of the fluorophore DY-490-NHS-ester (Dyomics, Germany) was mixed with 0.5 mM of the peptides in PBS (pH 7.4) and incubated for 24 h at room temperature. To block remaining DY-490-NHS-ester, 20 μL of a 1 M Tris/HCl solution (pH 7.4) was added, and the mixture was incubated for additional 24 h at room temperature. As a negative control the same protocol was used without peptide.

Fluorescence Microscopy. 2.5×10^4 HepG2 cells per well were seeded in a 96-well plate. After 48 h, the culture medium was removed, and 100 μL of the fluorescently labeled peptides or the uncoupled fluorophore was added. After 15 min, the cells were washed eight times with 200 μL of PBS. The cells were analyzed by fluorescence microscopy (fluorescence microscope CKX41, Olympus, Germany).

Statistical Analysis. All values for the ectodomain shedding assays are expressed as means ± standard error of the mean (SEM). The standard error values indicate the variation between mean values obtained from at least three independent experiments. Statistics were generated using one-way analysis of variance (one-way ANOVA) and Bonferroni multiple comparison posthoc test or calculated by Student's t test, using the online tool at http://www.physics.csbsju.edu/stats/t-test.html. P values <0.05 were considered statistically significant (indicated with *).

RESULTS

CANDIS Interacts with Membranes. CANDIS is a helical peptide with an amphipathic character (Figure 1A). In the first experiments we examined whether the peptide was able to interact with membranes. The secondary structure of the peptide was assessed by circular dichroism (CD) spectroscopy in the absence and presence of liposomes with different lipid compositions (Figure 1B). The helical content of CANDIS markedly increased from 37 to 73% in the presence of vesicles composed of 1-palmitoyl-2-oleoyl-*sn*-glycero-3-phosphocholine (POPC) and 1-palmitoyl-2-oleoyl-*sn*-glycero-3-phospho-L-serine (POPS) or POPC. However, the addition of cholesterol to both lipid compositions had a pronounced inhibitory effect on the binding of CANDIS toward lipid vesicles. The intrinsic fluorescence of the tryptophan residue (W10), permitted probing of the environment of this side chain that resided in the hydrophobic side of the α-helix. Figure 1C shows the intrinsic tryptophan fluorescence spectra in the absence and presence of liposomes with various lipid compositions. The increase of the fluorescence intensity and the shift to lower wavelengths clearly indicate that CANDIS binds to liposomes and that in the presence of liposomes the tryptophan side chain is buried in a hydrophobic environment. To prove that the CANDIS/liposome interaction is indeed mediated by hydrophobic interactions we performed the same experiments in the presence of high salt concentrations which should suppress ionic interactions (Figure 1C, right). The addition of 150 mM NaCl showed only marginal differences compared with the situation lacking salt, e.g., for the interaction of CANDIS with POPC vesicles. Furthermore, the CD spectra of CANDIS in interaction with POPC/POPS with and without salts showed comparable shapes, indicating that electrostatic interaction

DOI: 10.1021/acs.biochem.5b00497
Biochemistry 2015, 54, 5791−5801

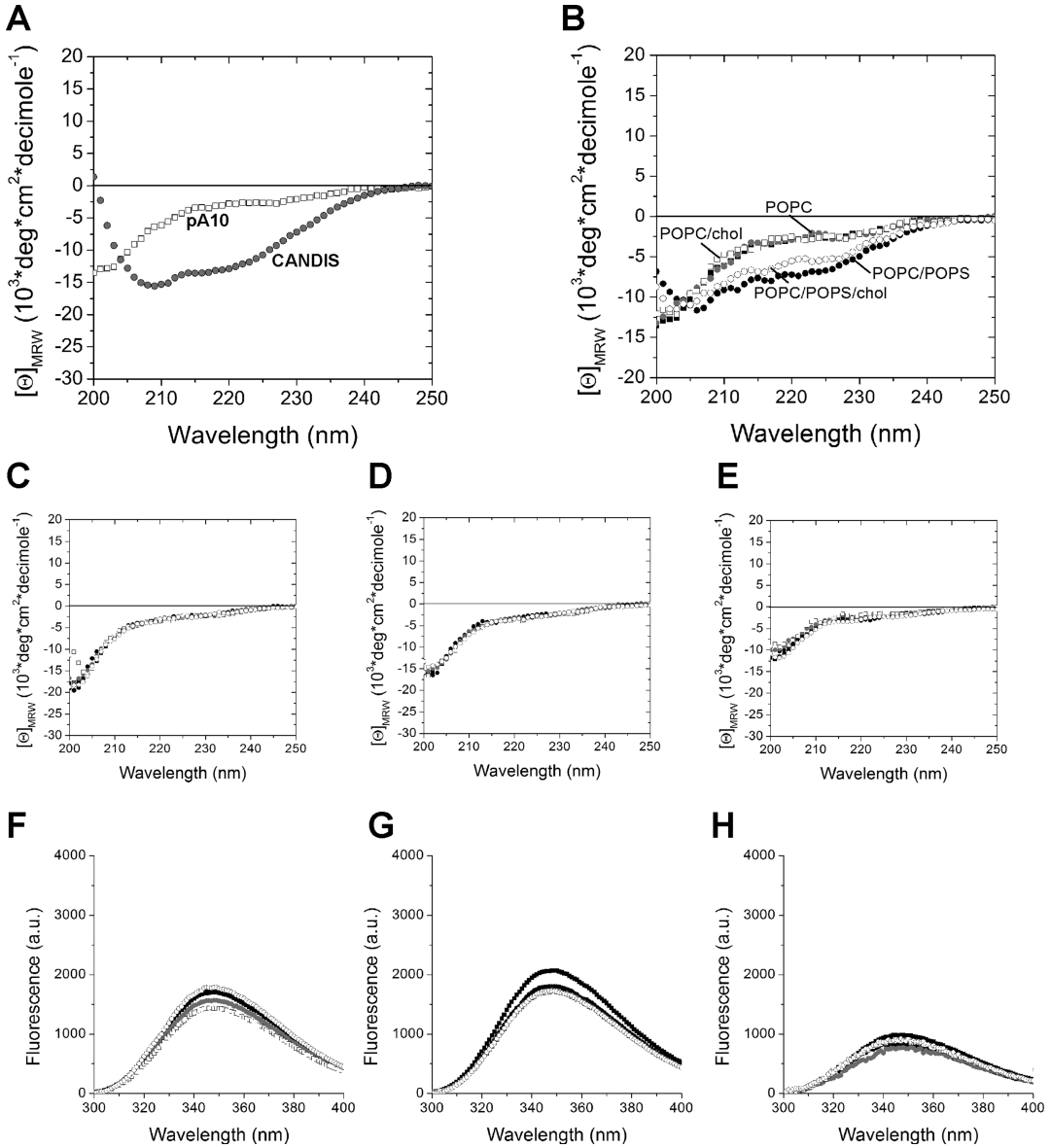

Figure 2. (A) CD spectra of the ADAM10 peptide (pA10, empty square) and the CANDIS peptide (gray filled circles) in solution at pH 7.4. (B) CD spectra of the ADAM10 peptide, (C) 2Q-CANDIS, (D) EE-CANDIS, and (E) 2R-CANDIS in the absence (empty squares) and presence of lipid vesicles composed of POPC/POPS (filled circles), POPC (gray circles), POPC/POPS/chol (filled squares), or POPC/chol (empty circles) in a P/L ratio of 1:48. The corresponding tryptophan emission fluorescence spectra were collected in a P/L ratio of 1:300 for (F) 2Q-CANDIS, (G) EE-CANDIS, and (H) 2R-CANDIS with the same lipid vesicles, respectively. Please note the varying scales on the *y*-axis compared to Figure 1C.

between the lipid head groups and the charged amino acids were not of major importance (Figure 1D). No difference in the interaction with POPC/POPS with and without salts was discerned, indicating that electrostatic interaction between the lipid head groups and the charged amino acids were not of major importance (Figure 1D).

To calculate the affinity of CANDIS–lipid interactions, dissociation constants (K_d) were determined by CD spectroscopy (Figure 1E). The changes in the overall secondary structural elements are indicative of a binding event of CANDIS upon stepwise addition of POPC/POPS or POPC vesicles with K_d values of 166 μM and 242 μM, respectively. The higher affinity for POPS containing vesicles was even more precisely determined by fluorescence spectroscopy. The conformational changes to helical contents of CANDIS upon membrane interaction might be influenced by the rigidity of the membrane, e.g., for cholesterol containing membranes. Therefore, we applied tryptophan emission fluorescence spectroscopy which is independent of structural changes upon membrane interaction. The insertion of the single indole ring into the membranes' hydrophobic environment presumably occurs prior to conformational changes of the whole peptide which leads to a lower dissociation constants as compared to CD measurements. Notably, the affinity for POPS containing membranes is 3-fold higher compared to POPC with K_d values of 52 μM and 174 μM, respectively (Figure 1F). The addition of cholesterol dramatically prevents peptide adsorption on the membrane surface with dissociation constants of 114 μM and 555 μM for POPC/POPS/chol and POPC/chol, respectively.

CANDIS Membrane Interaction Is Specific and the Hydrophobic Part Is Responsible for the Membrane Interaction. Whereas CANDIS is able to interact with

DOI: 10.1021/acs.biochem.5b00497
Biochemistry 2015, 54, 5791–5801

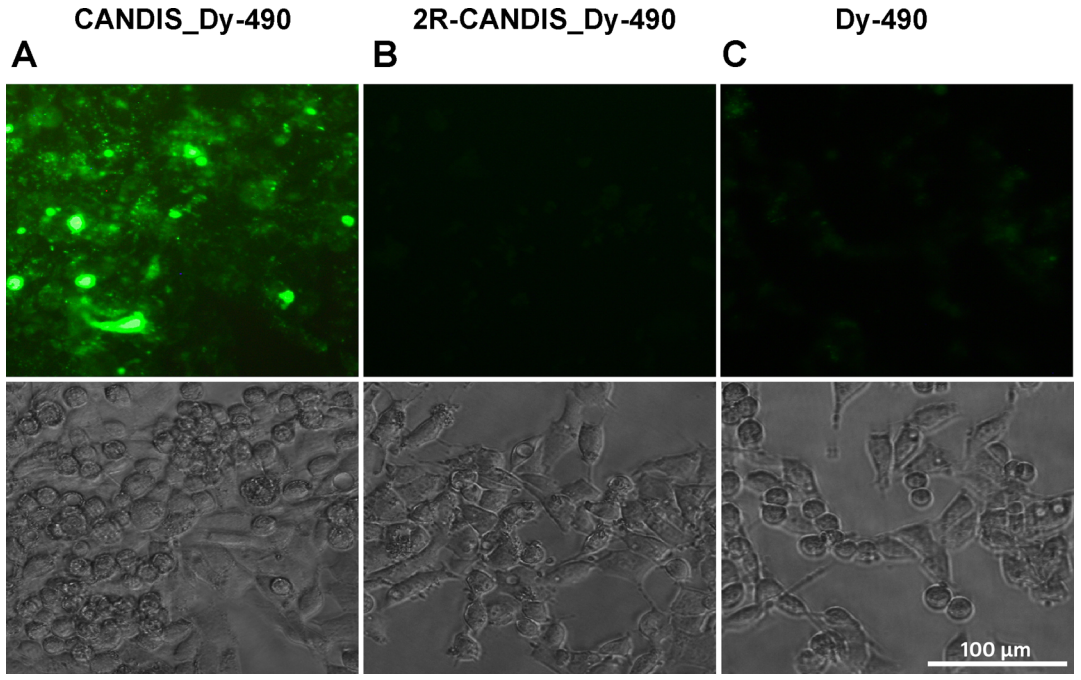

Figure 3. CANDIS interacts with HepG2 cells. HepG2 cells were incubated with CANDIS_Dy-490 (A), 2R-CANDIS_Dy-490 (B), or Dy-490 (C). Fluorescence was analyzed microscopically. The upper panel shows the fluorescence microscopy images, the lower panel the phase-contrast images.

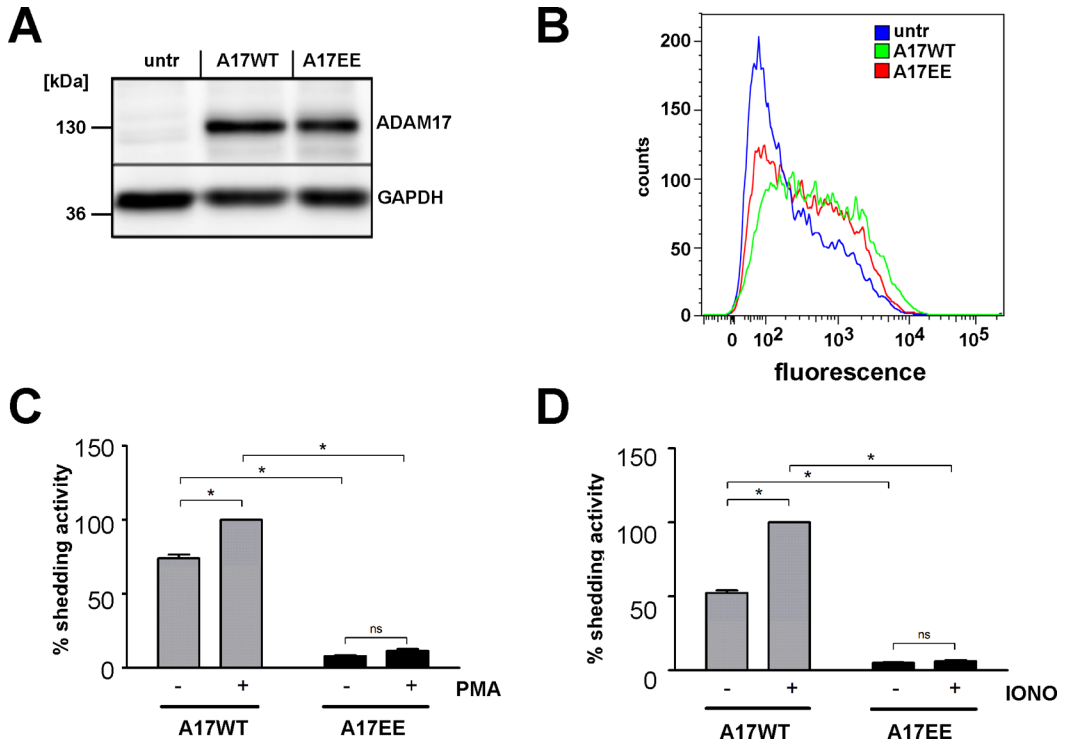

Figure 4. Expression and activity of the ADAM17EE mutant. (A) Western blot analysis of transfected ADAM10/17-deficient mouse embryonic fibroblasts (MEFs). Cells were transfected with either wild-type ADAM17 (A17WT) or ADAM17EE mutant (A17EE) and alkaline phosphatase-tagged TGF-α (TGF-α AP). Cell lysates were analyzed with anti-ADAM17 antibody. (B) Flow cytometric analysis of cell surface expression of wild-type ADAM17WT and ADAM17EE after transfection (blue: untransfected; green: WT ADAM17; red: ADAM17EE). (C and D) Shedding activity of the ADAM17EE mutant. Twenty-four hours after transfection with ADAM17 wild-type or mutant and TGF-α AP, MEFs were treated either with PMA for 2 h or with ionomycin for 30 min. Supernatants and cell lysates were collected and measured for alkaline phosphatase activity and baseline-corrected with AP activity of the controls. Shown is the relative AP activity in the supernatant compared to the total AP activity of supernatant plus cell lysates normalized to the stimulated wild-type ADAM17WT. The data show the mean of three independent experiments. (*p values < 0.05 indicating significance).

DOI: 10.1021/acs.biochem.5b00497
Biochemistry 2015, 54, 5791−5801

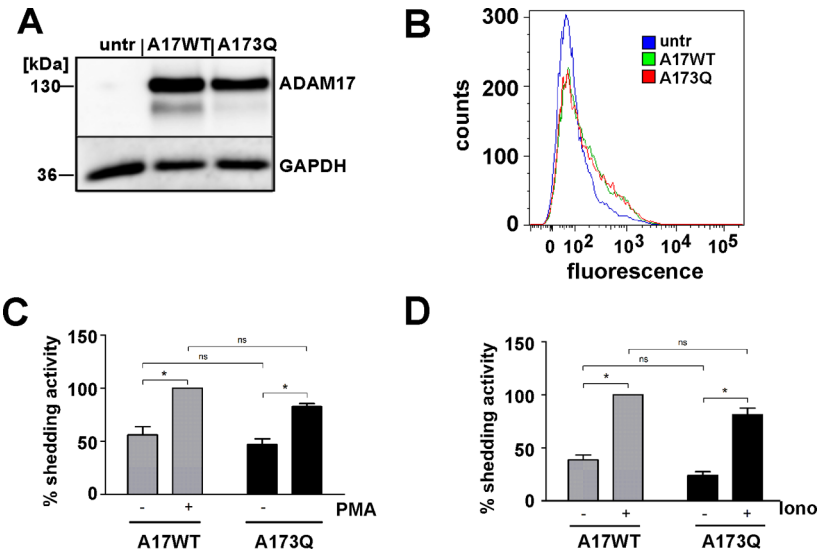

Figure 5. Expression and activity of the ADAM173Q mutant. (A) Western blot analysis of transfected ADAM10/17-deficient mouse embryonic fibroblasts (MEFs). The cells were transfected with TGF-α–AP and either wild-type ADAM17 (A17WT) or ADAM173Q mutant (A173Q). Cell lysates were analyzed with anti-HA antibody. (B) Flow cytometric analysis of cell surface expression of wild-type ADAM17WT and ADAM173Q after transfection (blue: untransfected; green: WT ADAM17; red: ADAM173Q) (C and D) Shedding activity of ADAM173Q mutant. Twenty-four hours after transfection with wild-type ADAM17WT or mutant and TGF-α AP, MEFs were treated either with PMA (C) for 2 h or with ionomycin (Iono) (D) for 30 min. Supernatants and cell lysates were collected and measured for alkaline phosphatase activity and baseline-corrected with the AP activity of the controls. The relative AP activity in the supernatant compared to the total AP activity of supernatant plus cell lysates normalized to the stimulated ADAM17WT is shown. The data show the mean of three independent experiments. (*p values <0.05 indicating significance).

ADAM17 substrates, the corresponding region of the closest relative ADAM10 is not.[15] In order to study whether the observed effects are specific for ADAM17, the corresponding region of ADAM10 was investigated. Figure 2A shows the comparison of the CD spectra of the ADAM10 peptide and CANDIS with large differences in the content of helical elements. Nevertheless, the peptide of ADAM10 showed CD spectra corresponding to small helical content. Furthermore, CANDIS exerted lipid binding properties accompanied by large conformational changes to 73% of helical content, whereas the ADAM10 peptide showed only less pronounced changes (7%) upon the same conditions (Figure 2B). Nevertheless, the changes in the CD spectra of the ADAM10 peptide in the presence of negatively charged PS containing vesicles showed that the peptide is principally able to interact with liposomes and that this interaction is enhanced with liposomes containing negatively charged lipids such as PS.

In order to study the influence of the hydrophobic side of the CANDIS helix we exchanged the two phenylalanine residues by two glutamine residues (2Q-CANDIS, Figure 2C), glutamic acids (EE-CANDIS, Figure 2D), or arginine residues (2R-CANDIS, Figure 2E). All these mutations completely destroyed the lipid binding properties of the peptide as monitored by CD spectroscopy. Furthermore, the lipid binding properties of mutated CANDIS peptides were examined by tryptophan emission fluorescence spectroscopy. Upon addition of POPC/POPS and POPC vesicles, the fluorescence intensity showed no alteration in fluorescence intensities or shifted emission maxima (Figure 2F–H). The disruption of the FWDF motif of CANDIS had therefore a dramatic impact on its key role in membrane binding events.

CANDIS Associates at the Eukaryotic Cell Membrane. Since model membranes of vesicles might not properly reflect the situation of a native eukaryotic cell membrane we tested whether CANDIS binds to membranes of living cells. Therefore, HepG2 cells were incubated with fluorescently labeled peptides and subsequently analyzed by fluorescence microscopy. Figure 3A shows that CANDIS associates at the plasma membrane of HepG2 cells, whereas the fluorescently labeled RR-CANDIS mutant (Figure 3B) nor the fluorophore alone did not (Figure 3C).

The Intact Hydrophobic Side of the CANDIS Helix Is Essential for ADAM17 Activity. In order to study the influence of the hydrophobic as well as the hydrophilic side of CANDIS on the proteolytic activity of ADAM17 we exchanged amino acid residues in these regions in the full-length molecule.

To analyze the importance of the hydrophobic region, we focused on our data gained from the experiments with the EE-CANDIS variant. We exchanged the two phenylalanine residues by glutamic acids in into the full-length molecule (A17EE) and studied the proteolytic activity of this ADAM17 mutant. ADAM10/ADAM17$^{-/-}$ MEF cells were transfected with cDNAs encoding for this variant and analyzed for expression by Western blot (Figure 4A). The variant and the wild-type molecule are expressed by the transfected cells. Cell surface expression of the wild-type and EE mutant was demonstrated by flow-cytometry analysis (Figure 4B). Cells were cotransfected with cDNA encoding for the TGFα-AP, and the shedding activity of this mutant was measured by AP activity in the supernatant of these cells in the presence and absence of PMA or ionomycin as ADAM17 stimulators. Figure 4C,D clearly shows that the A17EE mutant is completely inactive regardless of the presence of PMA or Ionomycin.

The hydrophilic (charged) side of the CANDIS helix contains three negatively charged amino acid residues which were exchanged against noncharged but still hydrophilic glutamines by mutation of the full-length ADAM17 (A173Q). Expression and cell surface expression was demonstrated by Western blot (Figure 5A) and flow-cytometry analysis (Figure 5B). The A173Q mutant showed no significant change in

DOI: 10.1021/acs.biochem.5b00497
Biochemistry 2015, 54, 5791–5801

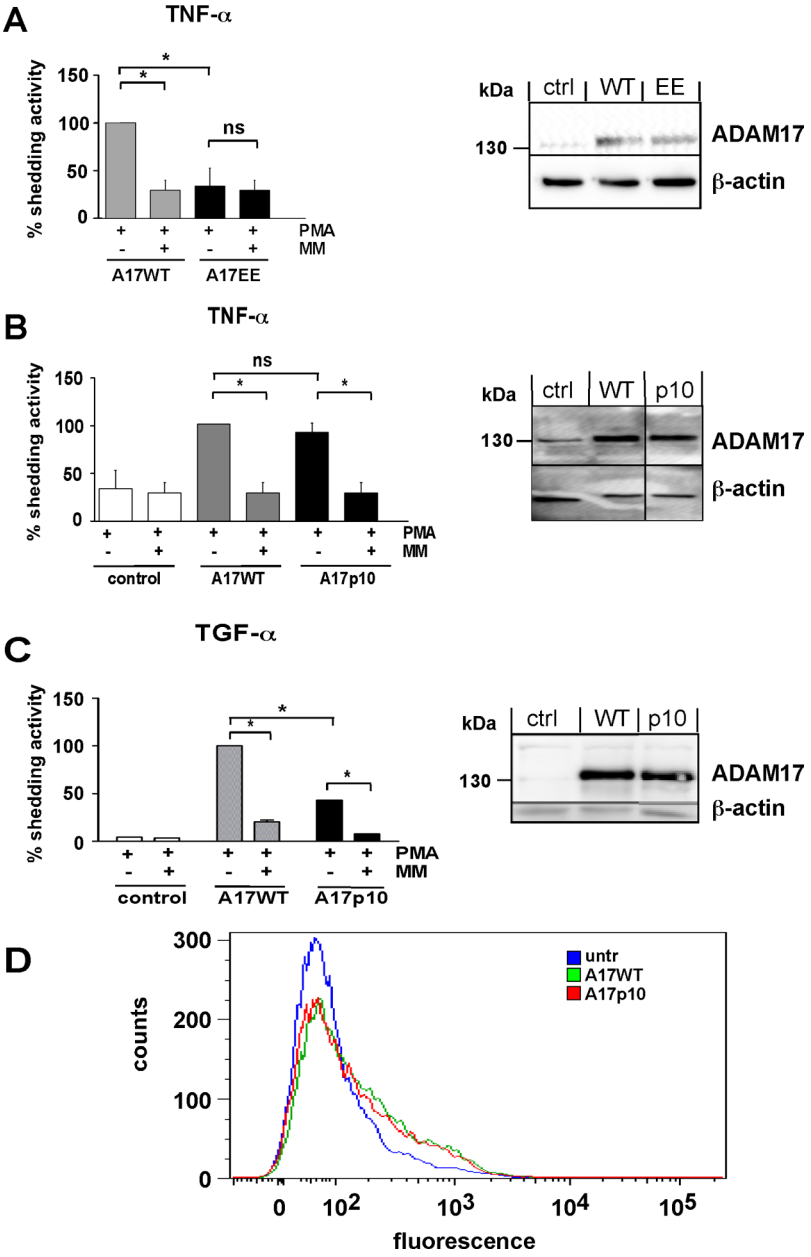

Figure 6. Analysis of TNF-α and TGF-α release by ADAM17 variants and ADAM17−CANDIS chimera. (A, left) Shedding of AP-tagged TNF-α is abrogated in the ADAM17EE variant. ADAM10/17-deficient mouse embryonic fibroblasts (MEFs) were cotransfected with extracellular AP-tagged TNF-α and wild-type ADAM17 or ADAM17EE variant. One day later, shedding activity was induced by the addition of PMA (+), and control cells were treated with PMA in the presence of the metalloprotease inhibitor Marimastat (MM). Cell lysates were analyzed with anti-HA antibody. In the normalization process, shedding activity in the stimulated sample transfected with wild-type ADAM17 was set to 100% of shedding activity. (A, right) Expression of C-terminal HA-tagged ADAM17 variants. (B, left) Consequences of CANDIS exchange within ADAM17 on TNF-α (B) shedding. Analogous to (A), cells were cotransfected with extracellular AP-tagged substrates and indicated ADAM17 variants and shedding activity stimulated 1 day post transfection. After 2 h, cells and supernatant were harvested and analyzed as described in the Materials and Methods section. (B, right) Expression of C-terminal HA-tagged ADAM17 variants. (C, left) Consequences of CANDIS exchange within ADAM17 on TGF-α shedding. Analogous to (A), cells were cotransfected with extracellular AP-tagged substrates and indicated ADAM17 variants and shedding activity stimulated 1 day post transfection. After 2 h, cells and supernatant were harvested and analyzed as described in the Materials and Methods section. (C, right) Expression of C-terminal HA-tagged ADAM17 variants (D) Flow cytometric analysis of cell surface expression of wild-type ADAM17WT and ADAM17p10 after transfection (blue: untransfected; green: WT ADAM17; red: ADAM17p10. FACS data for the ADAM17EE variant is shown in Figure 4. Shedding data show the mean of three independent experiments (*p values <0.05 indicating significance).

activity compared to the wild-type protease regardless of the presence of PMA (Figure 5C) or ionomycin (Figure 5D). From these data we concluded that the hydrophobic side of CANDIS and its ability to interact with membranes is essential for the shedding activity of ADAM17.

Influence of CANDIS Mutations on Other ADAM17 Substrates. The CANDIS peptide is able to bind to the type-I transmembrane molecules IL-6R and IL-1RII but not the type-II transmembrane protein TNF-α.[15] Therefore, we studied the influence of the EE mutation on the shedding of this molecule. Intriguingly, also shedding of this CANDIS-independent

DOI: 10.1021/acs.biochem.5b00497
Biochemistry 2015, 54, 5791−5801

ADAM17 substrate is abrogated in case the hydrophobic side of CANDIS is destroyed in the ADAM17EE mutant (Figure 6A). Since the corresponding peptide of ADAM10 showed also an interaction with liposomes, although less pronounced than CANDIS, we generated chimeric ADAM17 molecules in which the CANDIS was replaced by the corresponding region of ADAM10 (ADAM17p10). Figure 6B shows that the PMA stimulated shedding of TNF-α by the ADAM17p10 chimera is not changed compared to the wild-type, whereas TGF-α shedding (Figure 6C) is significantly reduced.

DISCUSSION

The major sheddase of many membrane-bound molecules, which are involved in regeneration processes and immune responses, is ADAM17. The release of growth factors, cytokines, and cytokine receptors from the cell surface catalyzed by this enzyme has to be tightly and efficiently controlled to minimize the risk of cancer progression and autoimmune diseases. The identification of a patient lacking ADAM17 and mice characterized by Chalaris et al. demonstrates that ADAM17 is important for protecting the skin and intestinal barrier.[2,3] In contrast, the absence or reduction of growth factor release from the cell surface by ADAM17 diminishes regenerative processes. Once activated, ADAM17 activity can be rapidly switched off by a PDI-mediated mechanism.[16,17] Interstingly, PDI mediated disulfide isomerization changes the isolated, flexible, elongated MPD structure into a rigid, compact conformation.[21] This conformational change controls the accessibility of substrates to the directly adjacent conserved region, which has been named CANDIS. In ADAM10, the closest relative of ADAM17, this region shows no homology to CANDIS. Although both proteases share some substrates, their regulation differs significantly.[30,31] In addition, the cleavage sites of ADAM10 and ADAM17 in the human IL-6R, a substrate of both proteases, are not identical, and the mode of substrate recognition appears to be different, since ADAM17's CANDIS is able to bind the human IL-6R, whereas the corresponding region of ADAM10 does not.[15]

Juxtamembrane segments appear to be essential regulatory elements in membrane proteins where these α-helical regions undergo structural changes and modulate the function of the full-length molecule. As described recently, the juxtamembrane segment in the epidermal growth factor receptor (EGFR) is essential for the activation of this receptor.[32,33] Although this intracellular EGFR element is neither functionally nor structurally related to the extracellular CANDIS region, these two examples point to such regions as novel and important regulatory elements.

It cannot be ruled out that CANDIS besides binding some ADAM17 substrates is also a general interaction hub for regulatory proteins. One candidate for such regulators are iRhoms, which are not only important for the transportation and maturation of ADAM17,[34−36] but seem also to play a relevant role in the substrate selectivity of ADAM17.[37]

Besides its property to bind to substrates, CANDIS is able to bind to membranes. By a combination of CD and tryptophan emission fluorescence the specific interaction of CANDIS to POPC and POPC/POPS containing vesicles could be shown. The lipid binding properties of CANDIS are independent of electrostatic interactions and are rather of hydrophobic nature. This interaction is presumably based on a two-step mechanism: The adsorption of the peptide is arranged by the FWDF motif, which is the driving force for anchoring the amphipathic peptide to the membrane. Exchange of amino acid residues in the hydrophobic side (e.g., 2Q-, 2R-, EE-CANDIS) abrogates lipid binding as evidenced by the lack of structural changes in the presence of lipid vesicles. Therefore, in a second step the changes to α-helical contents stabilize the localization of the peptide on the membrane. In the presence of cholesterol these binding events become disturbed leading to lower affinities accompanied by higher dissociation constants and less α-helical contents, probably due to the higher rigidity of the cholesterol containing membrane. Notably, cholesterol depletion of cells as well as phosphatidylserine exposure of apoptotic neutrophils lead to an increased shedding by ADAM17.[25,38] These results are in line with our data that phosphatidylserine enhances membrane binding of CANDIS, whereas the presence of cholesterol results in decreased membrane binding. Taken together, these data point to a sequence of events by which CANDIS is bound to the membrane and then leaves the membrane thereby facilitating substrate binding as a prerequisite for shedding. Although it remains speculative, this might be a mechanism by which the shedding activity of ADAM17 is regulated by the gradual increase in cholesterol levels along the exocytic pathway.[39]

The above-described lipid specific two-step mechanism of the CANDIS sequence has recently been observed for the mode of action of the anchoring sequence of the huntingtin protein, Htt17.[40] Here, the POPS-specific lipid interaction is highly dependent on hydrophobic phenylalanines and becomes disturbed by cholesterol. As the amphipathic Htt17 peptide has been shown to align on the surface of the membrane in a parallel orientation, it is feasible that the CANDIS orients parallel, too.

The importance of CANDIS for the activity of ADAM17 is underlined by the fact that mutations in CANDIS, which interfere with membrane binding of the peptide, completely abolished the enzymatic activity of the full-length molecule, whereas mutations at the hydrophilic site of the helix have no impact on the shedding activity of ADAM17. These results suggest that the membrane binding properties of CANDIS are an integral and important step toward the activation of ADAM17. Interestingly, besides TGF-α shedding, the shedding of the transmembrane type-II molecule TNF-α is also impaired, although CANDIS does not bind to TNF-α.[15]

ADAM17 is responsible for the generation of the most important initiators of immune responses, TNF-α and the soluble (s)IL-6R. Therefore, it is a key factor in the pathophysiology of autoimmune and chronic diseases and has a high potential as therapeutic target. Until now, there is no successful treatment with specific ADAM17 inhibitors targeting the active site. In the recent years several efforts have been undertaken to target so-called exosites. Tape et al. and others developed ADAM17 antibodies, which bind to extracellular parts of the enzyme, thereby inhibiting shedding activity.[41,42] Knowledge about the detailed role of MPD and CANDIS for different types of substrates is therefore of high value for the development of specific therapeutic interventions.

AUTHOR INFORMATION

Corresponding Author

*Phone +49 431 8801686. Fax +49 431 8805007. E-mail: jgroetzinger@biochem.uni-kiel.de.

Author Contributions

#S.D., M.M., and F.K. contributed equally.

DOI: 10.1021/acs.biochem.5b00497
Biochemistry 2015, 54, 5791−5801

Funding

This study was supported by the Deutsche Forschungsgemeinschaft (SFB 877, A4, A6), the RTG 1743 and the Excellence Cluster 306 'Inflammation at Interfaces'.

Notes

The authors declare no competing financial interest.

■ ACKNOWLEDGMENTS

The authors thank Lea Egli, Jonas Hiesner, Alina Lycke, and Jessica Schneider for their excellent technical assistance.

■ ABBREVIATIONS

AP, alkaline phosphatase; POPC, 1-palmitoyl-2-oleoyl-*sn*-glycero-3-phosphocholine; POPS, 1-palmitoyl-2-oleoyl-*sn*-glycero-3-phospho-L-serine; chol, cholesterol; SUV, small unilamellar vesicle; CANDIS, Conserved ADAM seventeeN Dynamic Interaction Sequence; ADAM, A Disintegrin And Metalloproteases; MPD, membrane-proximal domain; PMA, phorbol 12-myristate 13-acetate; Iono, ionomycin; AP, alkaline phosphatase; DMEM, Dulbecco's modified Eagle's medium; DMSO, dimethyl sulfoxide; IL, interleukin; TGF, transforming growth factor; TNF, tumor necrosis factor

■ REFERENCES

(1) Peschon, J. J., Slack, J. L., Reddy, P., Stocking, K. L., Sunnarborg, S. W., Lee, D. C., Russell, W. E., Castner, B. J., Johnson, R. S., Fitzner, J. N., Boyce, R. W., Nelson, N., Kozlosky, C. J., Wolfson, M. F., Rauch, C. T., Cerretti, D. P., Paxton, R. J., March, C. J., and Black, R. A. (1998) An Essential Role for Ectodomain Shedding in Mammalian Development. *Science 282*, 1281−1284.

(2) Chalaris, A., Adam, N., Sina, C., Rosenstiel, P., Lehmann-Koch, J., Schirmacher, P., Hartmann, D., Cichy, J., Gavrilova, O., Schreiber, S., Jostock, T., Matthews, V., Hasler, R., Becker, C., Neurath, M. F., Reiss, K., Saftig, P., Scheller, J., and Rose-John, S. (2010) Critical role of the disintegrin metalloprotease ADAM17 for intestinal inflammation and regeneration in mice. *J. Exp. Med. 207*, 1617−1624.

(3) Blaydon, D. C., Biancheri, P., Di, W. L., Plagnol, V., Cabral, R. M., Brooke, M. A., van Heel, D. A., Ruschendorf, F., Toynbee, M., Walne, A., O'Toole, E. A., Martin, J. E., Lindley, K., Vulliamy, T., Abrams, D. J., MacDonald, T. T., Harper, J. I., and Kelsell, D. P. (2011) Inflammatory skin and bowel disease linked to ADAM17 deletion. *N. Engl. J. Med. 365*, 1502−1508.

(4) Black, R. A., Rauch, C. T., Kozlosky, C. J., Peschon, J. J., Slack, J. L., Wolfson, M. F., Castner, B. J., Stocking, K. L., Reddy, P., Srinivasan, S., Nelson, N., Boiani, N., Schooley, K. A., Gerhart, M., Davis, R., Fitzner, J. N., Johnson, R. S., Paxton, R. J., March, C. J., and Cerretti, D. P. (1997) A metalloproteinase disintegrin that releases tumour-necrosis factor-alpha from cells. *Nature 385*, 729−733.

(5) Moss, M. L., Jin, S. L., Milla, M. E., Bickett, D. M., Burkhart, W., Carter, H. L., Chen, W. J., Clay, W. C., Didsbury, J. R., Hassler, D., Hoffman, C. R., Kost, T. A., Lambert, M. H., Leesnitzer, M. A., McCauley, P., McGeehan, G., Mitchell, J., Moyer, M., Pahel, G., Rocque, W., Overton, L. K., Schoenen, F., Seaton, T., Su, J. L., Becherer, J. D., et al. (1997) Cloning of a disintegrin metalloproteinase that processes precursor tumour-necrosis factor-alpha. *Nature 385*, 733−736.

(6) Scheller, J., Chalaris, A., Garbers, C., and Rose-John, S. (2011) ADAM17: a molecular switch to control inflammation and tissue regeneration. *Trends Immunol. 32*, 380−387.

(7) Moss, M. L., Jin, S. L., Becherer, J. D., Bickett, D. M., Burkhart, W., Chen, W. J., Hassler, D., Leesnitzer, M. T., McGeehan, G., Milla, M., Moyer, M., Rocque, W., Seaton, T., Schoenen, F., Warner, J., and Willard, D. (1997) Structural features and biochemical properties of TNF-alpha converting enzyme (TACE). *J. Neuroimmunol. 72*, 127−129.

(8) Reddy, P., Slack, J. L., Davis, R., Cerretti, D. P., Kozlosky, C. J., Blanton, R. A., Shows, D., Peschon, J. J., and Black, R. A. (2000) Functional analysis of the domain structure of tumor necrosis factor-alpha converting enzyme. *J. Biol. Chem. 275*, 14608−14614.

(9) Müllberg, J., Schooltink, H., Stoyan, T., Gunther, M., Graeve, L., Buse, G., Mackiewicz, A., Heinrich, P. C., and Rose-John, S. (1993) The soluble interleukin-6 receptor is generated by shedding. *Eur. J. Immunol. 23*, 473−480.

(10) Santos, D. O., Lorre, K., de Boer, M., and van Heuverswyn, H. (1999) Shedding of soluble receptor for tumor necrosis factor alpha induced by M. leprae or LPS from human mononuclear cells. *Nihon Hansenbyo Gakkai Zasshi 68*, 185−193.

(11) Bell, J. H., Herrera, A. H., Li, Y., and Walcheck, B. (2007) Role of ADAM17 in the ectodomain shedding of TNF-alpha and its receptors by neutrophils and macrophages. *J. Leukocyte Biol. 82*, 173−176.

(12) Rose-John, S. (2003) Interleukin-6 Biology is Coordinated by Membrane Bound and Soluble Receptors. *Acta Biochim. Pol. 50*, 603−611.

(13) Scheller, J., Chalaris, A., Schmidt-Arras, D., and Rose-John, S. (2011) The pro- and anti-inflammatory properties of the cytokine interleukin-6. *Biochim. Biophys. Acta, Mol. Cell Res. 1813*, 878−888.

(14) Jones, S. A., Scheller, J., and Rose-John, S. (2011) Therapeutic strategies for the clinical blockade of IL-6/gp130 signaling. *J. Clin. Invest. 121*, 3375−3383.

(15) Düsterhöft, S., Höbel, K., Oldefest, M., Lokau, J., Waetzig, G. H., Chalaris, A., Garbers, C., Scheller, J., Rose-John, S., Lorenzen, I., and Grötzinger, J. (2014) A disintegrin and metalloprotease 17 dynamic interaction sequence, the sweet tooth for the human interleukin 6 receptor. *J. Biol. Chem. 289*, 16336−16348.

(16) Bennett, T. A., Edwards, B. S., Sklar, L. A., and Rogelj, S. (2000) Sulfhydryl regulation of L-selectin shedding: phenylarsine oxide promotes activation-independent L-selectin shedding from leukocytes. *J. Immunol. 164*, 4120−4129.

(17) Willems, S. H., Tape, C. J., Stanley, P. L., Taylor, N. A., Mills, I. G., Neal, D. E., McCafferty, J., and Murphy, G. (2010) Thiol isomerases negatively regulate the cellular shedding activity of ADAM17. *Biochem. J. 428*, 439−450.

(18) Li, X., and Fan, H. (2004) Loss of ectodomain shedding due to mutations in the metalloprotease and cysteine-rich/disintegrin domains of the tumor necrosis factor-alpha converting enzyme (TACE). *J. Biol. Chem. 279*, 27365−27375.

(19) Wang, Y., Herrera, A. H., Li, Y., Belani, K. K., and Walcheck, B. (2009) Regulation of mature ADAM17 by redox agents for L-selectin shedding. *J. Immunol. 182*, 2449−2457.

(20) Düsterhöft, S., Jung, S., Hung, C. W., Tholey, A., Sönnichsen, F. D., Grötzinger, J., and Lorenzen, I. (2013) Membrane-proximal domain of a disintegrin and metalloprotease-17 represents the putative molecular switch of its shedding activity operated by protein-disulfide isomerase. *J. Am. Chem. Soc. 135*, 5776−5781.

(21) Düsterhöft, S., Jung, S., Hung, C. W., Tholey, A., Sönnichsen, F. D., Grötzinger, J., and Lorenzen, I. (2013) Membrane-proximal domain of a disintegrin and metalloprotease-17 represents the putative molecular switch of its shedding activity operated by protein-disulfide isomerase. *J. Am. Chem. Soc. 135*, 5776−5781.

(22) Tellier, E., Canault, M., Rebsomen, L., Bonardo, B., Juhan-Vague, I., Nalbone, G., and Peiretti, F. (2006) The shedding activity of ADAM17 is sequestered in lipid rafts. *Exp. Cell Res. 312*, 3969−3980.

(23) Parr-Sturgess, C. A., Rushton, D. J., and Parkin, E. T. (2010) Ectodomain shedding of the Notch ligand Jagged1 is mediated by ADAM17, but is not a lipid-raft-associated event. *Biochem. J. 432*, 283−294.

(24) Moreno-Caceres, J., Caja, L., Mainez, J., Mayoral, R., Martin-Sanz, P., Moreno-Vicente, R., Del Pozo, M. A., Dooley, S., Egea, G., and Fabregat, I. (2014) Caveolin-1 is required for TGF-beta-induced transactivation of the EGF receptor pathway in hepatocytes through the activation of the metalloprotease TACE/ADAM17. *Cell Death Dis. 5*, e1326.

DOI: 10.1021/acs.biochem.5b00497
Biochemistry 2015, 54, 5791−5801

(25) Matthews, V., Schuster, B., Schutze, S., Bussmeyer, I., Ludwig, A., Hundhausen, C., Sadowski, T., Saftig, P., Hartmann, D., Kallen, K. J., and Rose-John, S. (2003) Cellular cholesterol depletion triggers shedding of the human interleukin-6 receptor by ADAM10 and ADAM17 (TACE). *J. Biol. Chem. 278*, 38829−38839.
(26) Reiss, K., Cornelsen, I., Husmann, M., Gimpl, G., and Bhakdi, S. (2011) Unsaturated fatty acids drive disintegrin and metalloproteinase (ADAM)-dependent cell adhesion, proliferation, and migration by modulating membrane fluidity. *J. Biol. Chem. 286*, 26931−26942.
(27) Chen, G. C., and Yang, J. T. (1977) Two-point calibration of circular dichrometer with d-10-camphorsulfonic acid. *Anal. Lett. 10*, 1195−1207.
(28) Sreerama, N., Venyaminov, S. Y., and Woody, R. W. (2001) Analysis of protein circular dichroism spectra based on the tertiary structure classification. *Anal. Biochem. 299*, 271−274.
(29) Christiaens, B., Symoens, S., Vanderheyden, S., Engelborghs, Y., Joliot, A., Prochiantz, A., Vandekerckhove, J., Rosseneu, M., and Vanloo, B. (2002) Tryptophan fluorescence study of the interaction of penetratin peptides with model membranes. *Eur. J. Biochem. 269*, 2918−2926.
(30) Le Gall, S. M., Bobé, P., Reiss, K., Horiuchi, K., Niu, X. D., Lundell, D., Gibb, D. R., Conrad, D., Saftig, P., and Blobel, C. P. (2009) ADAMs 10 and 17 Represent Differentially Regulated Components of a General Shedding Machinery for Membrane Proteins such as TGF{alpha}, L-Selectin and TNF{alpha}. *Mol. Biol. Cell 20*, 1785−1794.
(31) Le Gall, S. M., Maretzky, T., Issuree, P. D., Niu, X. D., Reiss, K., Saftig, P., Khokha, R., Lundell, D., and Blobel, C. P. (2010) ADAM17 is regulated by a rapid and reversible mechanism that controls access to its catalytic site. *J. Cell Sci. 123*, 3913−3922.
(32) Choowongkomon, K., Carlin, C. R., and Sonnichsen, F. D. (2005) A structural model for the membrane-bound form of the juxtamembrane domain of the epidermal growth factor receptor. *J. Biol. Chem. 280*, 24043−24052.
(33) Hake, M. J., Choowongkomon, K., Kostenko, O., Carlin, C. R., and Sonnichsen, F. D. (2008) Specificity determinants of a novel Nck interaction with the juxtamembrane domain of the epidermal growth factor receptor. *Biochemistry 47*, 3096−3108.
(34) Adrain, C., Zettl, M., Christova, Y., Taylor, N., and Freeman, M. (2012) Tumor necrosis factor signaling requires iRhom2 to promote trafficking and activation of TACE. *Science 335*, 225−228.
(35) McIlwain, D. R., Lang, P. A., Maretzky, T., Hamada, K., Ohishi, K., Maney, S. K., Berger, T., Murthy, A., Duncan, G., Xu, H. C., Lang, K. S., Haussinger, D., Wakeham, A., Itie-Youten, A., Khokha, R., Ohashi, P. S., Blobel, C. P., and Mak, T. W. (2012) iRhom2 regulation of TACE controls TNF-mediated protection against Listeria and responses to LPS. *Science 335*, 229−232.
(36) Christova, Y., Adrain, C., Bambrough, P., Ibrahim, A., and Freeman, M. (2013) Mammalian iRhoms have distinct physiological functions including an essential role in TACE regulation. *EMBO Rep. 14*, 884−890.
(37) Maretzky, T., McIlwain, D. R., Issuree, P. D., Li, X., Malapeira, J., Amin, S., Lang, P. A., Mak, T. W., and Blobel, C. P. (2013) iRhom2 controls the substrate selectivity of stimulated ADAM17-dependent ectodomain shedding. *Proc. Natl. Acad. Sci. U. S. A. 110*, 11433−11438.
(38) Chalaris, A., Rabe, B., Paliga, K., Lange, H., Laskay, T., Fielding, C. A., Jones, S. A., Rose-John, S., and Scheller, J. (2007) Apoptosis is a natural stimulus of IL6R shedding and contributes to the pro-inflammatory trans-signaling function of neutrophils. *Blood 110*, 1748−1755.
(39) Kol, M. A., van Laak, A. N., Rijkers, D. T., Killian, J. A., de Kroon, A. I., and de Kruijff, B. (2003) Phospholipid flop induced by transmembrane peptides in model membranes is modulated by lipid composition. *Biochemistry 42*, 231−237.
(40) Michalek, M., Salnikov, E. S., and Bechinger, B. (2013) Structure and topology of the huntingtin 1−17 membrane anchor by a combined solution and solid-state NMR approach. *Biophys. J. 105*, 699−710.
(41) Tape, C. J., Willems, S. H., Dombernowsky, S. L., Stanley, P. L., Fogarasi, M., Ouwehand, W., McCafferty, J., and Murphy, G. (2011) Cross-domain inhibition of TACE ectodomain. *Proc. Natl. Acad. Sci. U. S. A. 108*, 5578−5583.
(42) Udi, Y., Grossman, M., Solomonov, I., Dym, O., Rozenberg, H., Moreno, V., Cuniasse, P., Dive, V., Arroyo, A. G., and Sagi, I. (2015) Inhibition mechanism of membrane metalloprotease by an exosite-swiveling conformational antibody. *Structure 23*, 104−115.

DOI: 10.1021/acs.biochem.5b00497
Biochemistry 2015, 54, 5791−5801